Department of Biomedical Sciences
University of Veterinary Medicine Vienna

Institute of Physiology, Pathophysiology and Biophysics

(Head: Univ.–Prof. Dr.med.vet. Dr.med. Reinhold Erben)

The Effects of Fibroblast Growth Factor 23 Inhibition in Wild-Type C57BL/6 and Klotho/Vitamin-D-Receptor Knockout Mice with Chronic Kidney Disease

Diploma Thesis

University of Veterinary Medicine Vienna

submitted by
Magdalena Piplits

Vienna, February 2023

Supervisor: Judith Radloff, PhD.
Institute of Physiology, Pathophysiology and Biophysics
Department of Biomedical Sciences
University of Veterinary Medicine Vienna

Reviewer: Ao.Univ.-Prof. Dipl.-Ing. Dr.agr. Thomas Kolbe
Institute of In-vivo and In-vitro Models
Department of Biomedical Sciences
University of Veterinary Medicine Vienna

Author’s Declaration:

I, Magdalena Piplits, hereby declare that this submission is entirely my own work, in my own words, and that all sources used in researching it are fully acknowledged and all quotations properly identified. It has not been submitted, in whole or in part, by me or another person, for the purpose of obtaining any other credit / grade.

Vienna, 09.02.2023

Table of Contents

1. Introduction

1.1. The Kidney

The kidneys are two bean-shaped organs, located on both sides of the spine in vertebrates. They are positioned retroperitoneal and can be found according to species in the lower thoracic to upper lumbar region. The kidneys play a crucial role as the filter system of our body and ensure that the homeostasis of numerous other systems, including the water and electrolyte balance, is maintained (Gille 2008).

Each kidney has a distinct convex and concave border, the latter being situated medially. This concave border features an indentation, the so-called *Hilus renalis,* which functions as the entry and exit way for blood vessels, nerves and the ureter. The renal hilum leads into an inner cavity (*Sinus renalis*), which contains the renal pelvis, as well as fat and the first segment of the ureter. The structure of the kidney is generally divided into lobes (*Lobi renales*). Each lobe contains two main components: the outer cortex and the inner medulla. These two components build the functional tissue, or parenchyma, of the kidneys. The tip (*Papilla renalis*) of each lobe ends in a widening, the calyx, which then empties into the renal pelvis and serves as the beginning of the ureter. A connective tissue capsule (*Capsula fibrosa*), as well as a thin layer of fat (*Capsula adiposa*), encompasses the surface of the tissue. These protective layers protect the kidneys from mechanical and thermal stimuli and help to internally fixate the position of the kidneys. Distributed throughout the medulla and cortex are nephrons – the functional units of the kidney. These blood-filtering microscopic structures are responsible for the production of urine. A nephron consists of two major components: the renal corpuscle and the renal tubule. The corpuscle serves as the beginning of the filtering system and is composed of a net of capillaries, the glomerulus, which is ultimately encapsulated by the Bowman's capsule. Each renal corpuscle possesses two poles at opposite ends. The vascular pole functions as the entry and exit way for afferent and efferent arterioles. The urinary pole serves as a passageway for the ultrafiltrate into the proximal tubule, the first segment of the tubule system (Gille 2008).

Primary urine originates as blood is filtered through the soluble walls of the capillaries. However, the endothelium of the capillaries holds back larger proteins and corpuscular elements of blood. This ultrafiltrate therefore consists mainly of water and soluble substances. After being filtered into the Bowman's capsule, the primary urine then flows into the next portion of the nephron, the renal tubule. The renal tubule system is composed of anatomically and functionally different segments (Gäbel and Fromm 2015):

1) The proximal tubule
    a. Proximal convoluted tubule
    b. Proximal straight tubule
2) The loop of Henle
    a. Descending loop
    b. Ascending loop
3) The distal convoluted tubule
4) Connecting tubule
5) Collecting ducts

The primary task of each of these components involves modifying the fluid by different mechanisms to convert primary urine to its final state. This entails reabsorption, secretion and excretion. Certain components, for example electrolytes, glucose and residual proteins, are removed, meaning they are reabsorbed from the tubules back into the blood. Water is also passively reabsorbed through the solvent drag mechanism. Additionally, other components like urea, uric acid, creatinine and electrolytes are added by means of active secretion from the blood into the tubules. At the end of this process, the urine, which is then emptied into the ureter, consists mainly of water, metabolic waste and toxins. Due to its key function in regulating water and electrolyte balance, as well as its role in the excretion of metabolic end products, the kidney is one of the most vascularized organs in the body. The kidneys receive approximately 20 % of cardiac output – this is an impressive amount considering their relatively small size. However, this large amount of blood supply is necessary, not only to supply the kidneys with sufficient nutrients and oxygen, but also to provide enough blood for

filtration and adequate transportation of substrates that have been reabsorbed or secreted by the tubule system (Gäbel and Fromm 2015).

The primary supply of blood originates from the renal arteries, *Arteria renalis*, which diverge directly from the abdominal aorta. Each renal artery enters the kidney at the renal hilum and then branches out into the renal sinus. Eventually, the network of arteries reaches the afferent arterioles, which feed into the glomeruli, where the blood now undergoes the filtration process. After filtration, the blood feeds into a network of veins identical to the layout of the arteries and proceeds to exit the kidney at the renal hilum. The blood supply that each glomerulus receives from its afferent arteriole provides the main driving force that is necessary for the filtering process. However, the afferent blood vessels are decoupled from the general circulatory regulation and are therefore able to regulate the blood pressure in the kidneys autonomously. Responsible for this auto regulation are two mechanisms: the Bayliss-Effect and tubuloglomerular feedback. The primary task of these mechanisms is to control the width of afferent blood vessels and consequently regulate renal blood flow. As a result, the rate of filtration, the glomerular filtration rate (GFR), remains largely independent of systemic blood pressure (Gäbel and Fromm 2015).

To grasp the far-reaching consequences that chronic kidney disease can have, it is first essential to understand which functions a physiological kidney possesses. The kidney has five major tasks:

1. The elimination of urinary metabolic end products and foreign substances. These substances can be exclusively filtered (for example, creatinine), filtered and partially reabsorbed (for example, urea), or filtered and additionally secreted (for example, potassium, uric acid, medication, toxins or drugs).
2. The conservation of substances that should remain within the body. These substances are either not filtered at all (for example, large-molecular proteins) or they are filtered and then reabsorbed (for example, glucose, amino acids and water).

3. The regulation of water and electrolyte balance through the excretion of concentrated or diluted urine, as well as through the adjustment of the excretion or absorption rate of individual electrolytes.
4. The regulation of acid-base balance through the excretion or reabsorption of protons.
5. Endocrine functions, such as the synthesis and secretion of erythropoietin and renin. The kidney plays a vital role in erythropoiesis, as well as in the systemic regulation of blood pressure. Additionally, the kidneys are responsible for the metabolisation of certain hormones, for instance, corticosteroids, testosterone and peptide hormones (Gäbel and Fromm 2015).

The essential function of excreting urinary end products, without losing other important substances, is perhaps one of the most difficult tasks. Excreted urinary substances are metabolic end products, which cannot be further broken down and can only be excreted in significant quantities by the kidneys. Generally, these products cannot be differentiated from other substances that should remain in the body based on molecular weight, substance class or electric charge. The kidneys use the following strategy to solve this task: filtration, reabsorption, secretion and excretion. It is crucial that tubule segments can reabsorb or secrete certain molecules. This includes ions like sodium, chloride, calcium and magnesium, but also other organic substrates like glucose and amino acids. To do so, each tubule segment consists of specialized cells that can ensure the transport of each specific substance. Initially, the glomerular capillaries filter all low-molecular solutes into the tubule system with the help of the glomerular filtration barrier. The filtration barrier consists of three layers: fenestrated endothelium, the basement membrane and podocytes. Molecules are allowed passage through this barrier based on their molecular size and electric charge. Small molecular solutes, as well as water, can flow freely, whereas substances with a larger molecular size, such as plasma proteins and blood cells, are prevented from passing through by the fenestrated endothelium. Particles with a molecular weight over 200 kDA are retained at the basement membrane, whereas the podocytes, the narrowest point of passage, retain all particles that are larger than 65 kDA. Tubular reabsorption then recovers all solutes, which the body still needs, by means of specific transport mechanisms. Conversely, due to secretion, certain solutes are transported back into the tubules. Ultimately, unabsorbed substances, as well as additionally secreted

solutes, now remain in the tubules and are excreted as urine. Depending on the animal species, up to one fifth of plasma flow is filtered in the glomeruli. However, only a little less than 1 % of the resulting filtrate is excreted as urine – this means that more than 99 % of filtrate is reabsorbed in the tubules and thus remains preserved in the body (Gäbel and Fromm 2015).

One of the most important parameters for assessing kidney function is the GFR. The GFR is defined as the volume filtered by kidney glomeruli per unit of time and therefore expresses the production rate of primary urine. It is commonly measured in milliliters per minute. The rate of filtration is dependent on the following factors (Gäbel and Fromm 2015):

1. The hydrostatic pressure, which represents the force that acts in the direction of the Bowman capsule.
2. The Bowman capsule tissue pressure, which acts as counter pressure against the forces of filtration.
3. The colloid osmotic pressure, or the osmotic pressure exerted by colloids (dissolved particles) in a solution. Large molecular proteins, which remain in the capillaries, create colloid osmotic pressure against the virtually protein free Bowman capsule space. This force therefore also works against filtration.

1.2. Chronic Kidney Disease

Chronic kidney disease (CKD) is a long-term, progressive, mostly irreversible impairment of kidney function that ultimately leads to kidney failure as a result of severely impaired filtration ability. Current guidelines characterize the term CKD by a GFR of less than 60 mL/min per 1·73 m^2, with the need for renal replacement therapy, meaning dialysis or kidney transplant (Webster et al. 2017). Currently, CKD poses an increasingly relevant health risk as the disease affects 10 % of adults worldwide (GBD 2015 Disease and Injury Incidence and Prevalence Collaborators 2016). All age groups and genders can be affected, but disease prevalence is more common in the elderly (Zhang and Rothenbacher 2008).

Due to progressive loss of kidney function, the complications of CKD can be very extensive and result in a variety of symptoms. The likelihood of cardiovascular disease and subsequent increased risk of death, as well as anemia and mineral and bone disease among other complications is significantly increased (Webster et al. 2017). The clinical signs of CKD can also include increased urine excretion and the occurrence of uremia. This is due to the loss of nephrons and the resulting decrease in GFR, which subsequently decreases the excretion of urinary end products. Products like creatinine, urea and uric acid can then be found in increased concentrations in serum (Andrukhova et al. 2018). Albuminuria, increased albumin in urine, is also a marker of kidney damage, which correlates to loss of kidney function (Eckardt et al. 2013). The resulting reduced quality of life and life expectancy emphasize the clinical and public health importance of patients suffering from CKD.

CKD is not only limited to humans, but also plays an important role in veterinary medicine. Estimates of prevalence in the domestic feline population can be found ranging from 1–3 % (Bartges 2012), or up to 50 % (Marino et al. 2014) when considering different factors, such as age and diagnostic standards. Prevalence in dogs was found to be less than 1 % with risk factors including age, body size and breed (Bartges 2012). Similar to CKD in humans, it is well known that CKD affects animal welfare negatively. Complications include hyperphosphatemia, hypokalemia, secondary renal hyperparathyroidism, anemia, proteinuria, systemic hypertension, metabolic acidosis, and uremia (Chakrabarti et al. 2012). Current therapeutic approaches focus on early recognition and diagnosis as well as kidney protective therapy aiming to prevent further nephron loss (O'Neill et al. 2013).

1.3. Fibroblast Growth Factor-23 and Klotho

Fibroblast growth factor-23 (FGF23) is a protein from the FGF family that plays an essential role in phosphate and vitamin D (1,25-Dihydroxyvitamin D) metabolism and regulation. Recent studies show that this biologically active hormone also plays a part in various other complex interactions with organs (Shimada et al. 2004, Rodelo-Haad et al. 2019).

There are 3 different subgroups in the FGF family, which are organized according to their function: the intracrine, the paracrine and the endocrine. FGF23 belongs to the endocrine subgroup, along with FGF19 and FGF21 (Hu et al. 2013). These endocrine hormones do not actually have a growth factor function, but control bile acid synthesis (FGF19), glucose and lipid metabolism (FGF21), as well as mineral homeostasis (FGF23) (Erben 2019). FGF23 can be produced in various tissues, however it is primarily secreted by osteocytes and osteoblasts (Martin et al. 2012). The mechanisms that regulate secretion are not fully understood, however, it is verified that FGF23 transcription is influenced by vitamin D hormone. Secretion can also be stimulated directly or indirectly by parathyroid hormone (PTH), phosphate, iron deficiency, proinflammatory cytokines, angiotensin II and aldosterone (Erben 2019).

All paracrine and endocrine factors bind to FGF receptors localized in cell membranes. However, in contrast to paracrine factors, the endocrine factors require an α- or β-klotho co-receptor to bind to a FGF receptor (Kurosu et al. 2006). α-klotho, hereafter referred to as klotho, is a transmembrane protein, which functions together with FGF receptor 1 as a receptor complex for FGF23 (Chen et al. 2018). Klotho is primarily expressed in the kidney, parathyroid and in the choroid plexus of the cerebral ventricle. Originally, this protein was not discovered in association with FGF23, but was believed to be a so-called “anti-aging gene” (Erben 2019). This assumption was based on the observation of the phenotype of klotho-deficient mice, which showed many characteristics of human aging, for example, a shortened life span, organ atrophy, vascular calcification and reduced bone mass. However, it was later recognized that FGF23 and klotho are part of the same signaling pathway. The observed “ageing” phenotype of klotho-deficient mice arises from an unleashed production of vitamin D hormone, which subsequently leads to hypercalcemia, hyperphosphatemia and vascular calcification (Erben 2019).

FGF23, also classified as a phosphaturic hormone, plays a vital role in regulating phosphate homeostasis and keeping serum levels balanced. In the proximal tubule, FGF23 inhibits phosphate reabsorption through several intermediate pathways, which ultimately leads to the reduction of sodium phosphate cotransporters in the luminal cell membrane (Erben 2019). In

addition, renal 1-α-hydroxylase, an enzyme responsible for creating biologically active vitamin D hormone (Zehnder and Hewison 1999), can be suppressed through FGF23 signaling. This specific effect is of extreme importance, as it cannot be compensated through other factors, and explains why FGF23 or klotho deficiency leads to unrestrained vitamin D hormone production (Erben 2019).

Calcitriol, also known as vitamin D hormone, is the biologically active form of vitamin D3 and belongs to the group of calciferols. Calciferols are steroid derivates that act as hormones, which explains the term "vitamin D hormone." The term vitamin D is inaccurate, as it is technically not a true vitamin per definition. Vitamin D3, also known as cholecalciferol, is produced in the skin when exposed to sunlight, however it does not have significant biological activity. It must first be hydroxylated in the liver and then again in the kidneys to form the biologically active form calcitriol $1,25(OH)_2D$. The biosynthesis of calcitriol is subject to strict regulation via the modulation of the expression of 1-α-hydroxylase in the proximal renal tubule, which can be activated by PTH and inhibited by FGF23, phosphate and calcitriol. Calcitriol helps regulate the body's calcium homeostasis, alongside parathyroid hormone and calcitonin. It can increase the serum calcium level through various mechanisms: 1) by increasing the renal or intestinal calcium absorption or 2) by increasing calcium mobilization from the bone. In addition, calcitriol can modulate the expression of sodium-phosphate cotransporters and thereby elevate the intestinal absorption of phosphate.

Klotho co-receptors can be found expressed in proximal and distal kidney tubules whereas the expression is significantly higher in the distal tubule (Andrukhova et al. 2012). The protein FGF23 can exert different effects depending on the location to which it binds. In the distal tubule, FGF23 can activate enzymes, so-called "with-no-lysine-kinases" (WNK) (Andrukhova et al. 2014), which are responsible for the regulation of certain ion channels and transport systems (Hoorn et al. 2011). Epithelial calcium channels (transient receptor potential channel subfamily vanilloid 5 (TRPV5)) and sodium chloride cotransporters are also activated, which stimulates calcium and sodium reabsorption (Andrukhova et al. 2014). The binding of FGF23 to receptors in the distal tubule therefore leads to the conservation of calcium and sodium.

The effects that FGF23 has on vitamin D metabolism – and subsequently on phosphate and calcium homeostasis – as well as the effects displayed in the proximal renal tubule, help clarify why klotho-deficient mice, where FGF23 has less affinity to bind, display the characteristic phenotype caused by hypercalcemia, hyperphosphatemia and vascular calcification. In summary, the FGF23/klotho complex functions as an essential safety net against hyperphosphatemia, by increasing phosphate excretion, in addition to indirectly inhibiting intestinal phosphate absorption, as well as calcium absorption, by suppressing vitamin D hormone synthesis. These mediated functions are summarized in Fig. 1.

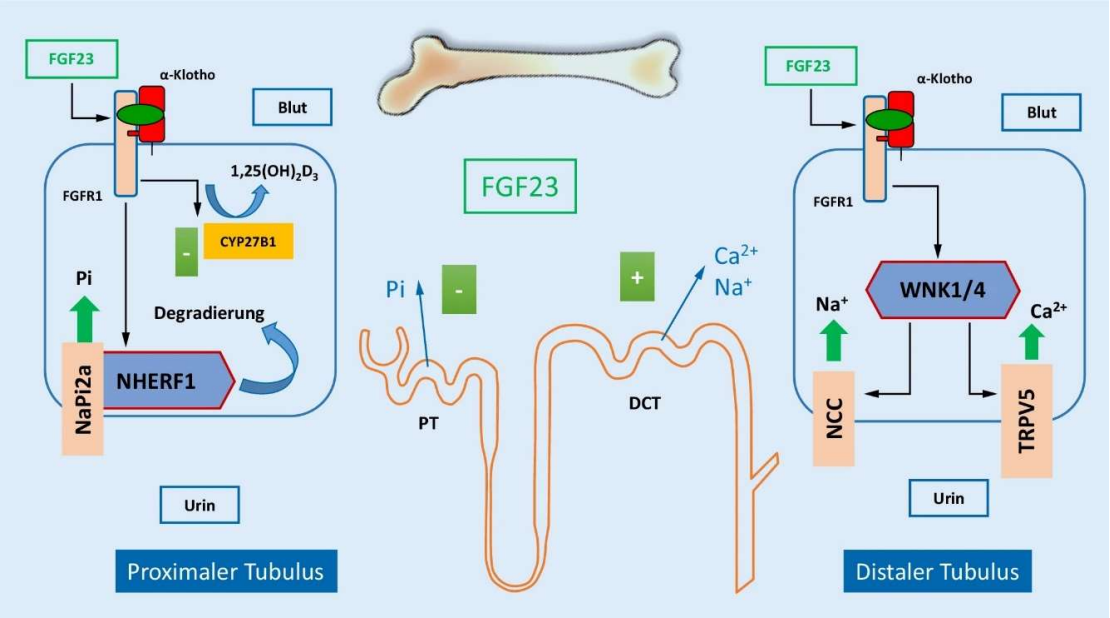

Fig. 1: FGF23/klotho kidney-bone-axis. In the proximal tubule (PT), the FGF receptor-1 (FGFR1)/klotho receptor complex suppresses 1-α-hydroxylase (CYP27B1), thereby inhibiting vitamin D hormone synthesis. Additionally, phosphate absorption is inhibited through several stages that cause the degradation of NHERF1 (responsible for sodium hydrogen exchange) with the sodium phosphate cotransporter (NaPi2a). In the distal tubule (DCT), the WNK1/4 complex is activated, which in turn activates the two transport systems NCC and TRPV5. The NCC transporter stimulates sodium absorption while the TRPV5 transporter stimulates calcium absorption (adapted: R.G. Erben, Attribution 4.0 International License (CC BY 4.0); https://link.springer.com/article/10.1007/s11560-019-0344-9/figures/1).

1.4. Fibroblast Growth Factor-23 and CKD

Studies have shown that the FGF23/klotho axis plays an essential role in the pathophysiology of CKD – namely that patients in all stages of CKD show increased blood concentration levels of FGF23. This increase in FGF23 is one of the first biomarkers known to indicate disease progression in patients. Generally, the greater the loss of kidney function, the more significantly FGF23 increases in blood (Isakova et al. 2012). High levels of circulating FGF23 have not only been associated with general disease progression and subsequent mortality, but also an increased cardiovascular risk due to chronic complications like vascular calcification and cardiac hypertrophy (Isakova et al. 2011). The declining GFR, due to advancing loss of kidney function, has other far-reaching negative effects. The decrease in GFR leads to decreased renal phosphate excretion, which in turn leads to hyperphosphatemia. Hyperphosphatemia, as previously mentioned, once again stimulates FGF23 secretion from the skeleton (Andrukhova et al. 2014). It is verified that increased levels of FGF23 are a significant risk factor for mortality in CKD patients, however, the mechanisms that lead to this early increase of FGF23 in blood are still unclear (Isakova et al. 2011).

1.5. Aim of the study

The FGF23/klotho axis plays a central role in the pathophysiology of CKD. The aim of this study was to investigate the role of klotho in correlation with renal fibrosis, as well as how acute FGF23 inhibition affects wild-type, vitamin-D-receptor (VDR) knockout and klotho/vitamin-D-receptor knockout mice in an experimental CKD model. This study therefore focuses on the following hypotheses:

1. Klotho assumes a protective role in the kidney and can reduce the extent of renal fibrosis in a CKD model in wild-type, VDR knockout and VDR/klotho knockout compound mice.
2. Acute inhibition of FGF23 influences the amount of renal fibrosis in a CKD model in wild-type, VDR knockout and VDR/klotho knockout compound mice.

To investigate these topics further, histological and molecular biological methods were used. As part of a large-scale project, it was also relevant to find out whether resulting effects are klotho-dependent or independent. The results should provide more insight on the pathophysiology of the FGF23/klotho signaling pathway in CKD.

2. Materials and Methods

2.1. Animals

All animal procedures were approved by the Ethical Committee of the University of Veterinary Medicine Vienna, as well as the Austrian Federal Ministry of Science and Research, and are compliant with European guidelines for animal experiments (Directive 2010/63/EU) *(license number BMWF_68.205/0054-II/3b/2013).*

The mouse model is suitable for examining pathophysiological processes that mimic structural and functional changes in human kidney disease. To understand certain effects, the mice can also be genetically modified. In the case of this thesis, knockout mice were used, meaning that the genes of interest were specifically deactivated.

In this study, n = 46 mice were examined. Male mice with a C57BL/6 genetic background were used and divided into nine groups. The following genotypes were used: wild-type (wt/wt//wt/wt), vitamin D receptor deficient mice (wt/wt//-/-) and klotho/vitamin D receptor deficient mice (-/-//-/-). Wild-type mice will hereafter be referred to as wt/wt, vitamin D receptor deficient mice as wt/-- and klotho/vitamin D receptor deficient mice as --/-- for simplification while reading. Each genotype was then either sham operated (SH) or 5/6 nephrectomized (NX). SH mice served as control groups. Eight weeks after surgery, three additional NX groups of each genotype were given a single 10 μg intravenous injection of anti-FGF23 antibody (FGF23AB). All other groups were given a control antibody (vehicle). Blood and tissue samples were then removed four hours after the injection. Tab. 1 summarizes the respective groups with regard to the genotype, the type of operation, the injected antibody and the size of each cohort.

Tab. 1: Overview of experimental setup

Group	Genotype	Surgery	Treatment	Number of Animals (n)
1	wt/wt	SH	Vehicle	5
2	wt/wt	NX	Vehicle	5
3	wt/--	SH	Vehicle	6
4	wt/--	NX	Vehicle	5
5	--/--	SH	Vehicle	5
6	--/--	NX	Vehicle	5
7	wt/wt	NX	FGF23AB	5
8	wt/--	NX	FGF23AB	5
9	--/--	NX	FGF23AB	5

As mentioned previously, it is established that loss of function klotho mice exhibit an aging-like phenotype, which is primarily due to unregulated vitamin D metabolism. Other pathologies include hypercalcemia, ectopic calcification of blood vessels, secondary hyperparathyroidism, hypogonadism, hypoglycemia, pulmonary emphysema and atrophy of skin and other tissues. After approximately three weeks of age, these mice stop growing and typically die at eight to nine weeks of age due to their abundant pathologies (Kuro-o 2009). The concurrent effects of increased vitamin D metabolism can be prevented by specific knockout of VDR (Kuro-o 2009). To provide those animals with a balanced mineral supply, they are fed a “rescue diet” (RD) (Sniff, Soest, Germany), which is enriched with 2.0 % calcium, 1.25 % phosphate, 20 % lactose and 600 IU of vitamin D per kilogram to help normalize mineral homeostasis. VDR/klotho knockout compound mutant mice that are maintained on this diet show normal life expectancy (Erben et al 2002). However, when given to wt/wt mice, this diet has been shown to exacerbate CKD due to the high calcium and phosphate content (Lau et al. 2013). On the one hand, RD helps keep VDR knockouts viable, but on the other hand, can also worsen renal injury in wt/wt mice.

Ad libitum access to water and RD was allowed. The mice were held in groups of at least two animals at 22–24 °C with a 12 hour light/12 hour dark cycle.

2.2. 5/6 Nephrectomy

5/6 nephrectomy (5/6NX), also known as the subtotal nephrectomy, is an established method to induce chronic renal failure in rodents. This experimental model mimics chronic kidney disease by removing a large amount of organ mass (Lim et al. 2014). There are different approaches to the 5/6NX, one being the ligature model and the other the ablation model, whereas the ligature model is predominately used in rats. In principle, one kidney is always completely removed, combined with a partial infarction or amputation of the two poles of the second kidney. An additional possibility is the combination of these two methods. As a result of this treatment, symptoms of CKD develop in mice. The insufficient amount of functional kidney tissue leads to hyperfiltration and consequent glomerular und tubular damage. The 5/6NX can therefore also be classified as a hyperfiltration model. The widespread glomerulosclerosis und tubulointerstitial fibrosis of the kidney tissue results in the loss of physiological function (Lim et al. 2014).

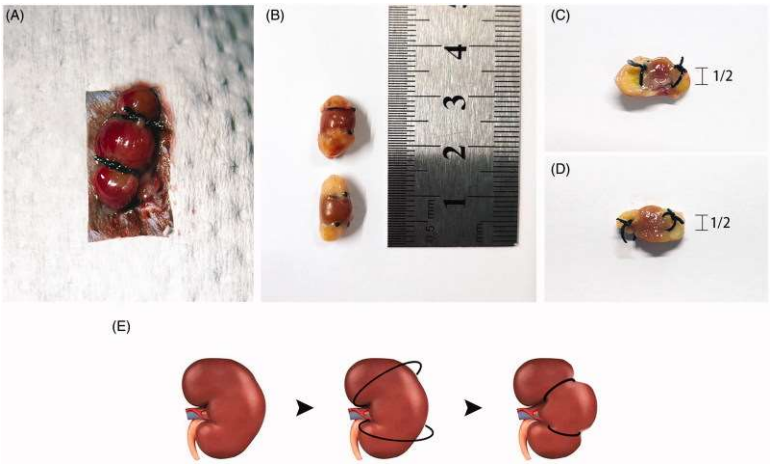

Fig. 2: Surgical execution of a 5/6 nephrectomy (5/6NX). (A) shows the surgical placement of the ligatures on each kidney pole. The subsequent necrosis due to the ligature can be seen in (B). Ligature coils should be half the diameter of the kidney in order to create a successful ligature and avoid bleeding (C, D). A schematic overview of a 5/6NX can be seen again in (E) (adapted: Rui-Zhi T. et al. Attribution 4.0 International License (CC BY 4.0); https://www.ncbi.nlm.nih.gov/pmc/articles/PMC6598497/figure/F0001/).

To establish identical conditions in NX and SH groups, SH mice were also operated. An established method for the SH operation consists of the exposure and repositioning of one kidney initially, followed by the second kidney one week later, so that postoperative trauma and pain management are identical in both groups. An intraperitoneal injection of ketamine and medetomidine (17/0.08 mg/kg) initiated anesthesia for the surgery and maintenance of anesthesia was ensured by isoflurane (2 %). Buprenorphine and metamizole were administered subcutaneously as pre-surgical analgesic management. Post-surgical analgesic management was managed with metamizole for 3 days and after thorough consideration of each animals status also with buprenorphine. Both groups were euthanized eight weeks after surgery with an intraperitoneal injection of ketamine (50 mg/kg) and medetomidine (0.25 mg/kg). Various samples, including both kidneys, were taken and shock frozen or further prepared for histological analysis.

2.3. Histology

An overview of all dyes, solvents and powders that were required for histological processing and staining can be found in Tab. 2.

During necropsy, the removed kidneys were freed from their tissue capsule, as well as any additional blood vessels, before they were divided into two halves. One half was used for histological examination and the other for molecular biological testing. The tissue for histological examination was then fixed in 4 % paraformaldehyde for 24 hours before being embedded in paraffin. The tissue for molecular biological testing was snap frozen in liquid nitrogen and stored at -80 °C.

The paraffin blocks were sectioned at 5 µm using the Microm HM355S rotary microtome (Thermo Fisher Scientific, USA) and placed into a paraffin floating bath (MEDAX, Germany). The slices were then transferred onto an object slide coated with 3-Aminopropyltriethoxysilane (APES) (Sigma-Aldrich, USA) to increase the adhesion of the sections to the glass surface of the slide. Prior to staining, each slide was dewaxed by means of a descending alcohol series as described in Tab. 3.

Tab. 2: Dyes, solvents and powders used for histological processing and staining

Dyes, solvents and powders	**Manufacturer**
Xylol	
Paraffin	
Isopropanol	
3-Aminopropylthriethoxysilane	Sigma-Aldrich
Hematoxylin	Merck KGaA
Sodium iodate (NaIO3)	Fluka Analytical
Aluminum potassium sulfate dodecahydrate (KAI(SO4)2)	Merck KGaA
Chloral hydrate (C2H3Cl3O2)	VWR Chemicals
Citric acid (C6H8O7)	Merck KGaA
Eosin G	Merck KGaA
Glacial acetic acid	Merck KGaA
Direct Red 80 (Sirius Red F3B)	Sigma-Aldrich
Picric acid solution (1,2 %)	AppliChem GmbH
Hydrogen chloride (37 %)	Merck KGaA
DePeX	SERVA Electrophoresis

Tab. 3: Overview of dewaxing protocol

Solutions	**Duration**
Xylene I	15 min
Xylene II	15 min
Isopropanol	5 min
70 % Ethanol	5 min
40 % Ethanol	5 min
dH2O	5 min

The dewaxed and dried sections were then stained according to the picrosirius red (PSR) staining protocol shown in Tab. 4. PSR staining is a histological technique specifically designed to display collagen fibers in tissue, even very small amounts of collagen can be detected (Montes and Junqueira 1991). This is essential for determining if a pathological amount of collagen, meaning fibrosis, is present and to which degree. The PSR solution stains collagen fibers red, whereas muscle fibers and cytoplasm are stained yellow (Lattouf et al. 2014). The staining solution was prepared by combining 0.5 g Sirius Red F3B (Sigma-Aldrich, USA) and 500 mL of saturated aqueous picric acid solution (AppliChem, Germany). The finished PSR staining solution is very stable and can be used for several months. However, PSR stained sections must be evaluated within 14 days of staining, as the stained sections are photosensitive. The slides should therefore also be stored away from light (Montes and Junqueira 1991).

Tab. 4: Overview of PSR staining protocol

Dyes and Solutions	**Duration**
Picrosirius red	90 min
Acidified Water I	3 min (protected against light)
Acidified Water II	3 min (protected against light)
Isopropanol I	3 min
Isopropanol II	3 min
Xylol I	7 min
Xylol II	7 min

The stained kidney sections were analyzed using an Axioscope 50 microscope (Carl Zeiss Microscopy, Germany) along with the Axiocam color 503 microscope camera (Carl Zeiss Microscopy, Germany). The microscope settings were standardized and set to 20 x magnification, an exposure time of 3.2 ms and the light intensity regulator was on position ten. Four photographs were taken per slide of the PSR stained sections. A certain distance to the surgically scarred kidney tissue was ensured as well as the avoidance of blood vessels in each photographed quadrant. The focus while photographing the cortex was on the glomeruli. The amount of collagen in each image was then analyzed using semi-automatic Image J

software (open source). A threshold value was determined to distinguish between two types of pixels. The ratio between collagen stained area and total tissue area was calculated.

2.4. Western blotting

Western blotting refers to the transfer of proteins to a carrier membrane, which can then later be detected and analyzed based on antigen-antibody interaction (Hnasko and Hnasko 2015). It entails extracting and quantifying total protein in each sample, gel electrophoresis, blotting and then detection. First, the protein in each sample was extracted and quantified via bicinchoninic acid assay (BCA assay). The BCA assay is a biochemical method used to quantitatively measure total protein in samples. The method is based on the combination of the biuret reaction with BCA, which enables the colorimetric detection of proteins (Smith et al. 1985). Samples were first prepared by homogenizing half of one kidney mixed with 300 µl of radioimmunoprecipitation assay buffer (RIPA buffer) (0.05 mol/l Tris (pH 7.4/HCl), 0.15 mol/l NaCl, 1 M EDTA, 1 % Triton X-100, 1 % sodium deoxycholate, 0.1 % sodium dodecyl sulphate (SDS)). Protease inhibitors (cOmplete^{TM} ULTRA Tablets and PhosSTOP^{TM}, Roche Applied Science, Germany) were also added to the RIPA buffer prior to homogenization with the FastPrep–24 5G homogenizer (MP Biomedicals, China).

The reagent solution was then freshly prepared from the BCA assay kit (Pierce^{TM} BCA Protein Assay Kit, ThermoFisher Scientific, USA) stock solutions. The standards as well as the samples were pipetted as duplicates into a 96 well microtiter plate. The plate was then heated in a thermo shaker (neoLab, Germany) for 30 minutes at 37 °C and mixed at 400 rpm. Protein absorbance was then detected with the EnSpire 2300 multilabel reader spectrophotometer (PerkinElmer, USA) at a wavelength of 562 nm. The protein concentration of each sample was calculated according to a bovine serum albumin (BSA) standard curve.

Sodium dodecyl sulfate – polyacrylamide gel electrophoresis (SDS-PAGE) is an analytical biochemical method, developed by Ulrich K. Laemmli, used to separate substances according to their molecular mass by means of an electric field (Laemmli 1970). Self-mixed and poured

polyacrylamide gels were used for electrophoresis. Additional materials and equipment that were required for the SDS-PAGE have been specified in Tab. 5 and Tab. 6.

Tab. 5: Equipment for SDS-PAGE

Equipment	**Terminus**	**Manufacturer**
Electrophoresis mini-tank	Mini-PROTEAN Tetra System	Bio-Rad Laboratories
Heating block	Thermo mixer block thermostate	Science services
Pipettes	eppendorf research plus	Eppendorf
Voltage source	Electrophoresis power supply EV 231	Consort
Vortexer	Vortex genie	Scientific Industries, Inc.

Tab. 6: Materials for SDS-PAGE

Materials	**Manufacturer**
Casting stand gasket	Bio-Rad Laboratories
Electrode assembly	Bio-Rad Laboratories
Gel casting frame	Bio-Rad Laboratories
Gel casting stand	Bio-Rad Laboratories
Pipette tips	VWR Collection
SDS gel combs	Bio-Rad Laboratories
Serological pipettes	TPP Techno Plastic Products AG
Short plates	Bio-Rad Laboratories
Spacer plates (0.75mm)	Bio-Rad Laboratories

Samples were prepared by mixing the calculated protein concentration, which was determined according to the previously mentioned BCA assay, with the respective amount of NaCl and 15 µl of loading buffer (0.1 mol/l Tris (pH 6.8), 10 % glycine, 4 % SDS, 4 % β-mercaptoethanol, 0.2 % bromophenol blue). Samples were incubated and denatured at 97 °C for ten minutes using a heating–thermomixer (Science Services, Germany) and subsequently centrifuged and vortexed before loading. For electrophoresis, 10 µg of each sample was loaded at 50 µg of total protein per well. A protein ladder marker (Precision Plus Protein™ Dual Color Standards, Bio-Rad Laboratories, USA) was also loaded onto the gel, thus enabling the estimation of protein size in the samples. The SDS-PAGE was run in the "Mini-PROTEAN Tetra System" (Bio-Rad Laboratories, USA) in electrophoresis buffer (60.58 g Tris, 288.24 g glycine, 20 g SDS) for 30 minutes at 80 V initially, then at 120 V for 90 minutes.

Following the SDS-PAGE, gels and filter paper (Thermo Fisher Scientific, USA) were soaked in nitrocellulose blotting buffer (6.06 g Tris, 28.84 g glycine, 400 ml methanol; volume adjusted to 2 L with diH_2O) and then transferred onto Amersham Protran nitrocellulose membranes (Cytiva, USA) using a semi-dry blotting chamber (PEQLAB Biotechnologie, Germany). The equipment and material that was required for western blotting can be found in Tab. 7.

Tab. 7: Equipment and material for western blotting

Equipment and material	**Terminus**	**Manufacturer**
Blotting chamber	Semi dry blotter	PeqLab Biotechnologie
Filter paper	Thermo Fisher Scientific	Filter paper
Nitrocellulose membrane	Amersham Protran nitrocellulose western blotting membrane	Cytiva
Voltage source	Electrophoresis power supply EV 231	Consort

After blotting for 90 minutes at 14 V, membranes were stained with Ponceau S to proof successful protein transfer, then destained in distilled water and placed into blocking solution (tris-buffered saline (TBS) (0.05 mol/l Tris (pH 7.4/HCl), 0.15 mol/l NaCl, 0.05 % Tween-20, 0.02 % Thimerosal) containing 2 % BSA overnight at 4 °C. Following blocking, membranes were incubated in primary and secondary antibodies as well as loading controls, which can be found in Tab. 8. The membranes were washed three times for 15 minutes in washing solution (TBS, 0.05 % Tween-20) between each antibody application.

Tab. 8: Overview of antibodies for immunodetection

Primary antibody	**Manufacturer**	**Dilution**	**Incubation**
Anti-Human klotho Monoclonal Anitbody	TransGenic Inc.	1:1000	4 °C overnight
Secondary antibody	**Manufacturer**	**Dilution**	**Incubation**
Anti-Rat IgG	Sigma-Aldrich	1:1000	Room temperature 1 h
Anti-Rabbit IgG	Cell Signaling Technology, Inc.	1:1000	Room temperature 1 h
Anti-Mouse IgG	Sigma-Aldrich	1:5000	Room temperature 1 h
Loading control	**Manufacturer**	**Dilution**	**Incubation**
Anti-β-Actin Monoclonal Antibody	Sigma-Aldrich	1:5000	Room temperature 1 h

To visualize the specific signals, the membranes were then incubated in Clarity™ Western ECL Blotting Substrate (Bio-Rad Laboratories, USA) for three minutes. The pictures for analysis were taken with a Chemi-Doc-It™ 600 Imaging System (UVP, UK) and protein signal was then quantified using LI-COR software (LI-COR Biotechnology, USA). The protein expression of anti-klotho antibodies was normalized to anti-β-Actin.

2.5. Statistical Analysis

Statistical evaluation was performed using GraphPad Prism Version 8 software (GraphPad Software, USA). Picrosirius red histological data was analyzed with a two-way analysis of variance (ANOVA) followed by a Student-Newman-Keuls (SNK) multiple comparison test. The fixed factors were genotype and treatment. Western blot analysis was performed with an unpaired T-Test. Expression of the target proteins was normalized to the previously mentioned loading controls. For all tests, P values ≤ 0.05 (*) were considered significant and data is presented as mean ± standard error of mean (SEM). Grubbs' test was performed to remove outliers.

3. Results

3.1. Evaluation of PSR Staining

To gain more insight about the role of FGF23 signaling in CKD related renal fibrosis, PSR staining of the kidney sections was used for histological evaluation. Renal fibrosis was evaluated for three different genotypes: wild-type, VDR knockout and VDR/klotho knockout mice, respectively SH or NX operated, as well as for vehicle and FGF23AB groups. In Fig. 3, a histological representation of renal fibrosis for each genotype and treatment can be found. A graphical representation of the according percentages of renal fibrosis for each group is summarized in Fig. 4.

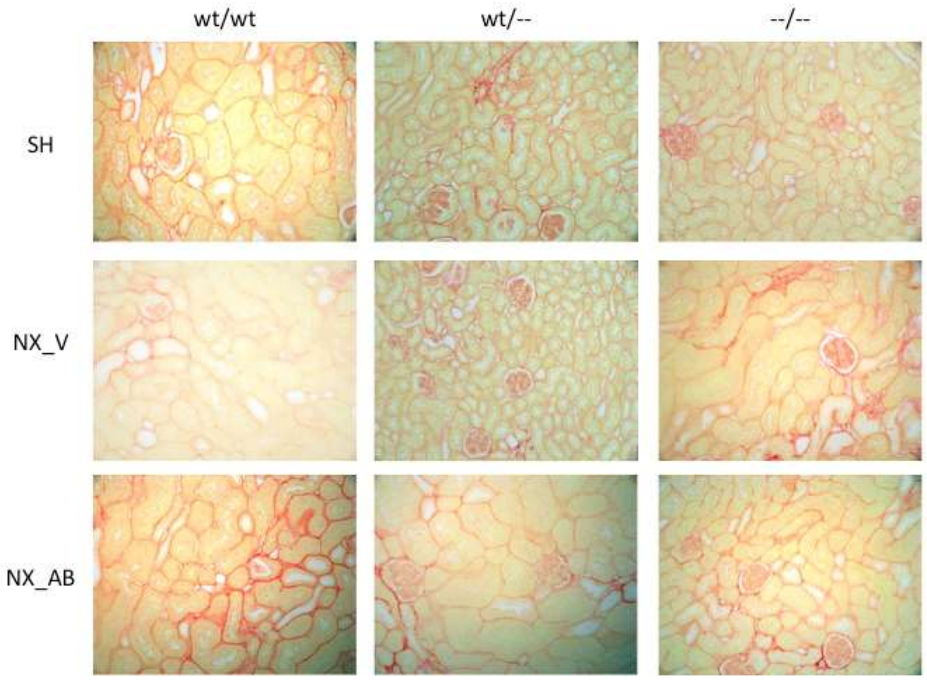

Fig. 3: Histological representation of renal fibrosis after staining with picrosirius red in wt/wt, wt/-- and --/-- after undergoing sham surgery (SH) or 5/6 nephrectomy (NX) and or treatment with anti-FGF23 antibody (AB).

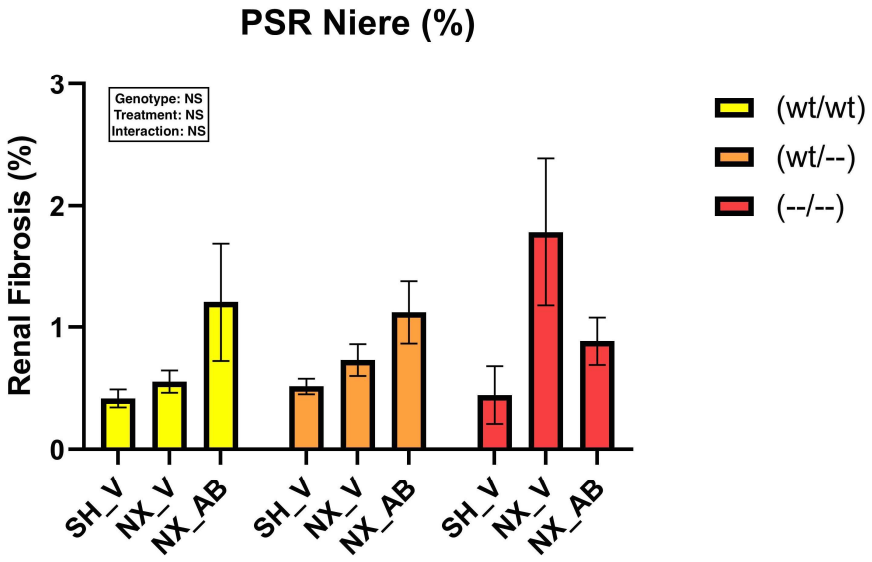

Fig. 4: Graphical representation of renal fibrosis (in %) after picrosirius red staining in wt/wt, wt/-- and --/-- after undergoing 5/6 nephrectomy (NX) or sham surgery (SH). Animals were classified as vehicles (V) or treated with an anti-FGF23 antibody (AB). Data was analyzed with a two-way ANOVA followed by a Student-Newman-Keuls multiple comparison test. Data represents the mean ± SEM of 4-6 animals in each group.

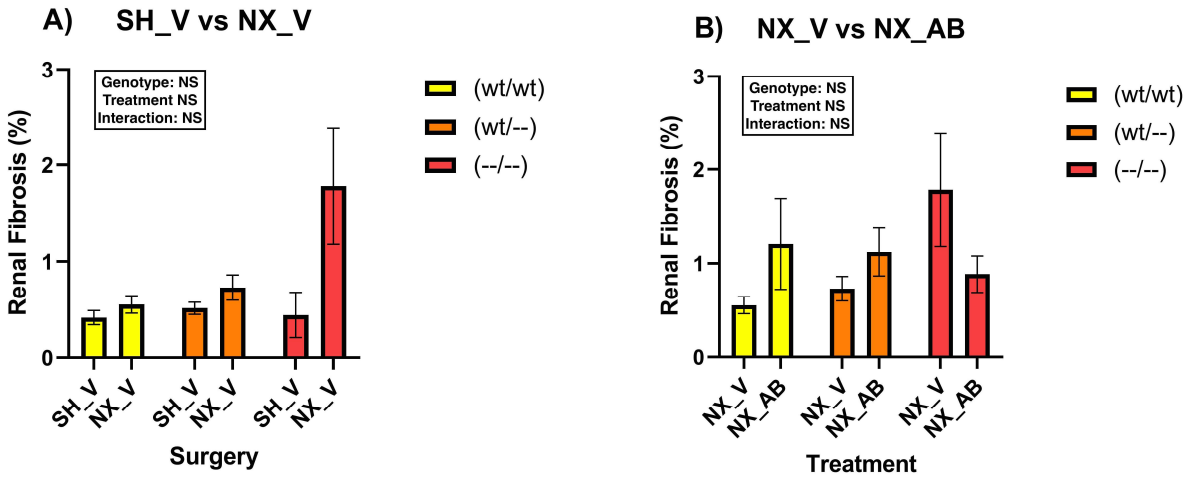

Fig. 5: Graphical comparison of renal fibrosis (in %) after staining with picrosirius red in wt/wt, wt/-- and --/-- mice. Animals were 5/6 nephrectomized (NX) or sham operated (SH) and were classified as vehicles (V) or treated with an anti-FGF23 antibody (AB). **A)** Comparison between vehicle animals that were either NX or SH operated. **B)** Comparison of NX operated that were either vehicles or AB treated. Data was analyzed with a two-way ANOVA followed by a Student-Newman-Keuls multiple comparison test. Data represents the mean ± SEM of 4-6 animals in each group.

Statistical evaluation revealed that genotype does not have a modifying effect on the amount of renal fibrosis. In Fig. 5, SH vehicle and NX vehicle mice were compared to assess if the surgical procedure itself influenced renal fibrosis. In general, a significant effect of FGF23 antibody treatment, or a role played by genotype or surgery could not be observed in our results.

3.2. Evaluation of Western Blotting

To further investigate the behavior of klotho expression in wt/wt, wt/-- and --/-- mice, as well as the effects of FGF23 inhibition in these respective groups, we examined klotho protein expression via western blot analysis. The samples were divided into nine groups based on genotype (wt/wt, wt/-- and --/--), surgery (SH or NX) and antibody treatment (FGF23AB).

The klotho antibody protein expression results are summarized in the bar charts found below in Fig. 6, according to surgery type, and in Fig. 7, according to antibody treatment.

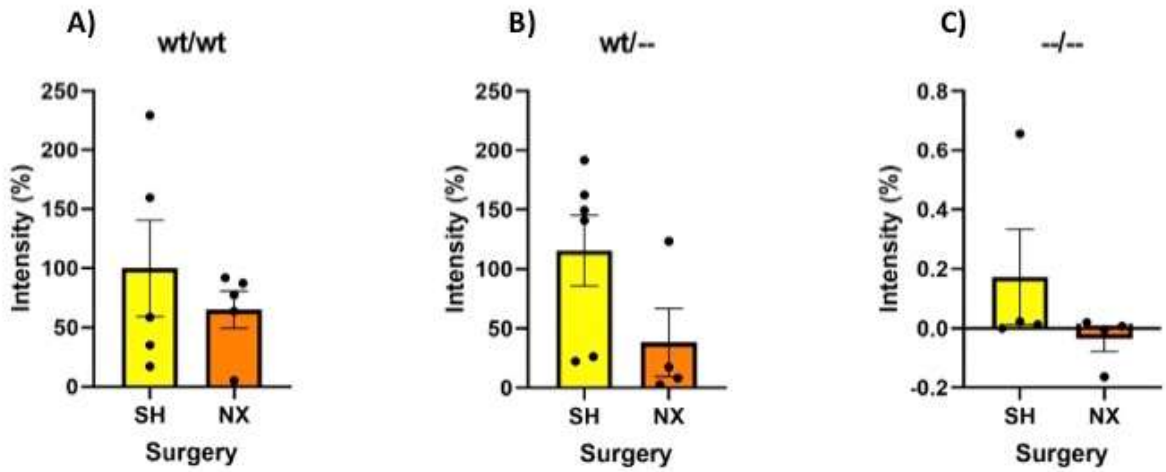

Fig. 6: Graphical bar chart comparison of klotho antibody protein expression in intensity (%) after western blot analysis of target protein according to genotype **A)** wt/wt, **B)** wt/-- and **C)** --/-- as well as based on surgery type: 5/6 nephrectomized (NX) or sham operated (SH). Statistical analysis was performed via an unpaired T-Test. Presented data is shown as mean ± SEM with 4-6 animals in each group.

Statistical evaluation revealed that 5/6NX did not significantly lower the expression of klotho. However, we can see that the general effect of surgical procedure was similar regardless of genotype. As can be seen in Fig. 6, the graphs also confirm that our VDR/klotho knockouts were successful, as klotho intensity is very minimal in the SH group and even less in the NX group.

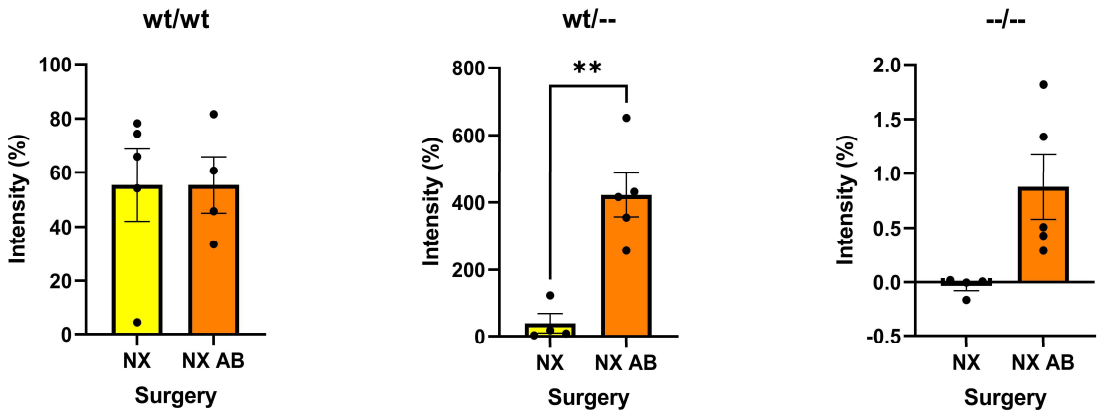

Fig. 7: Graphical bar chart comparison of klotho antibody protein expression in intensity (%) after western blot quantification of target protein according to genotype **A)** wt/wt, **B)** wt/-- or **C)** --/-- in 5/6 nephrectomized (NX) mice. Vehicles were compared to mice treated with anti-FGF23 antibody (NX AB). Statistical analysis was performed via an unpaired T-Test. Presented data is shown as mean ± SEM with 4-6 animals in each group. ** $P < 0{,}01$.

When observing the effect that FGF23 antibody application had on different genotypes, as can be seen in Fig. 7, analysis showed that there was no significant effect on the production of klotho in the wt/wt group. On the contrary, the wt/-- group showed a significant increase ($p < 0.01$) in klotho production after FGF23 antibody application, as did the --/-- group. Though the klotho intensity in the --/-- mice is technically statistically significant, we consider the amount of klotho to be so minimal that we have disregarded this as biologically relevant and have not marked it in the graphs. A sample excerpt of the western blots expressing klotho protein signal can be found in Fig. 8. To be noted in Fig. 8A is the strong klotho signal presented by an --/-- animal, which can most likely be explained through human error, for example, through false genotyping or a mix-up during the western blot process. This particular signal was therefore ignored during the evaluation of results.

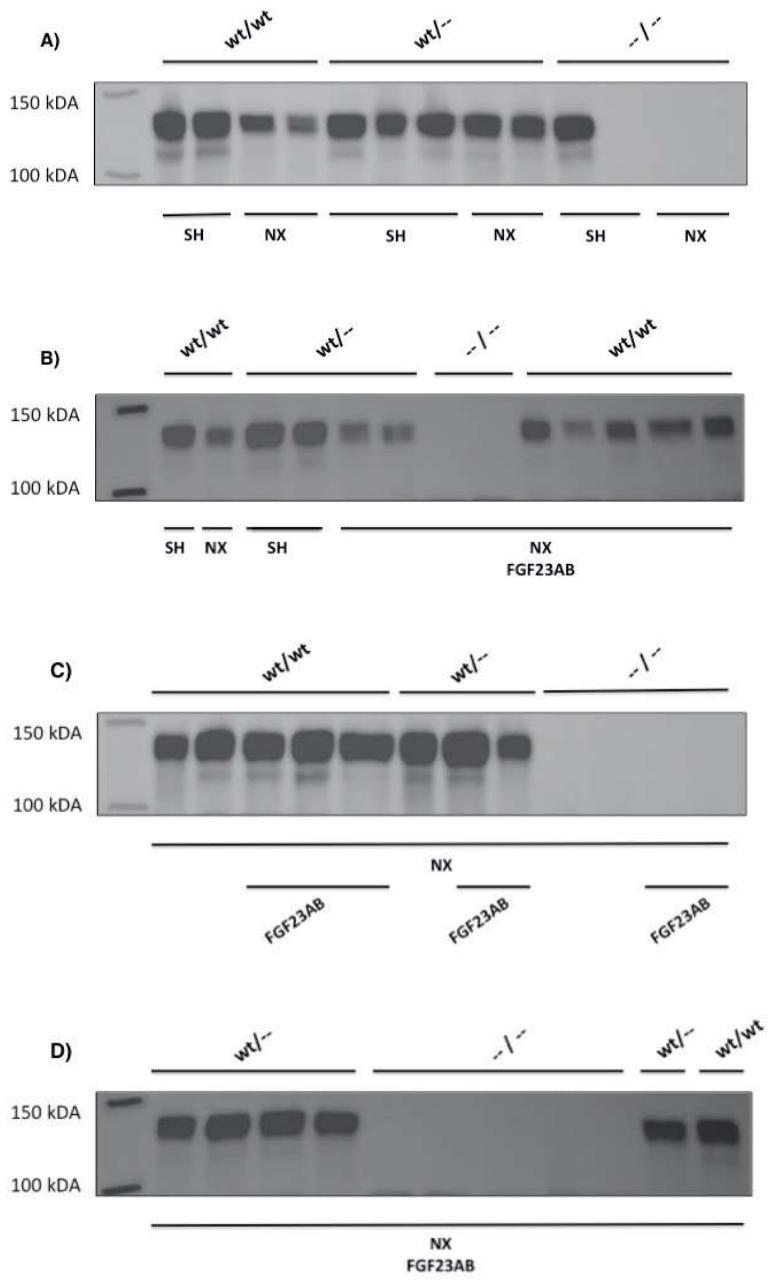

Fig. 8: Sample excerpt of relative klotho protein expression in western blot analysis. Bands are labeled according to genotype (wt/wt, wt/--, --/--), surgery type (SH or NX) and treatment (FGF23AB). **A)** Comparison of klotho expression in SH or NX animals of all genotypes. **B)** Comparison of NX animals treated with FGF23AB of all genotypes to SH or NX vehicle animals of genotypes wt/wt and wt/--. **C)** Comparison of vehicles and FGF23AB treated animals that were NX operated of all genotypes. **D)** Comparison of NX FGF23 animals of all genotypes.

4. Discussion

In 1997 Kuro-o et al discovered a mutation in the mouse klotho gene, which led to a process that was similar to ageing. Klotho deficient mice displayed symptoms of early lethality as well as hyperphosphatemia, hypercalcemia and hypervitaminosis D (Kuro-o et al. 1997). Kuro-o et al laid the building blocks for countless research exploring the relationship between FGF23, klotho and vitamin D. Klotho, a co-receptor for FGF23, can be primarily found in the distal tubule of the kidneys and the plexus choroideus in the brain (Andrukhova et al. 2012). The klotho/FGF23 complex can suppress vitamin D hormone synthesis as well as phosphate reabsorption (Erben 2019). VDR is expressed in most other tissues along with the kidneys and is essential in regulating calcium homeostasis as well as the synthesis of vitamin D hormone (Wang et al. 2012).

We aimed to investigate the interaction between klotho, renal fibrosis and acute FGF23 blockage in wt/wt, wt/-- and --/-- mice with C57Bl/6 background. In order to mimic CKD induced fibrosis, animals were 5/6 nephrectomized (5/6NX). 5/6NX is one of the most frequently used models in rodents, which is based on the loss of organ mass to mimic progressive renal failure. This reduction of organ mass consequently leads to hyperfiltration, oxidative stress and inflammation as well as tubular atrophy, glomerulosclerosis and interstitial fibrosis. The C57BL/6 genetic background has proven to be more resistant to the development of fibrosis in comparison to other strains (Bao et al. 2018). This strain-dependent resistance can be overcome by the application of a calcium and phosphate enriched diet (Radloff et al. 2021). Renal fibrosis, characterized by widespread tubulointerstitial fibrosis and glomerulosclerosis, is the “final manifestation of chronic kidney disease” and has far-reaching consequences, which are severely detrimental to overall kidney function (Cho 2010). Renal fibrosis is always the ultimate result of CKD – making it an excellent prognostic indicator – and there are numerous cellular and molecular mechanisms that lie behind this pathophysiological process. Once CKD progresses to its end stage, the need for dialysis and or kidney transplantation is unavoidable (Cho 2010). Therefore, an improved understanding of CKD pathogenesis is pertinent to establish a basis for future pharmacological intervention.

Numerous recent studies have shown that klotho assumes a protective role in the kidney against fibrosis. Wu et al. investigated, among other things, the role of TRPC6 in relation to renal fibrosis along with the effect of administering soluble klotho to wild-type and *Trpc6*-knockout mice. They found that the application of soluble klotho alleviated renal fibrosis caused by unilateral ureter obstruction in wild-type mice (Wu et al. 2017). Other studies have also confirmed that klotho plays an important role "protecting tubular cells … as a senescence suppressor" (Maique et al. 2020) and has a positive effect on renal function by ameliorating renal fibrosis (Miao et al. 2021). Therefore, in this work, the relationship between klotho, FGF23 and renal fibrosis was investigated. Fibrosis is defined as a pathological increase of connective tissue as a result of exo- or endogenous damaging stimuli, for example inflammation or circulatory impairment. This accumulation of extracellular matrix and fibroblasts in place of functioning parenchyma eventually leads to the hardening of the affected organ and ultimately to the restriction of respective organ function. This is a process that takes place over the course of several weeks or months (Cho 2010).

Firstly, statistical evaluation of our results revealed that genotype plays no significant role in the progression of fibrosis. Overall, there was no difference between wild-type mice and knockouts, or between klotho knockouts and klotho/VDR knockouts. A potentially interesting development would have been a significant difference between klotho and klotho/VDR knockouts, suggesting that the klotho co-receptor, or rather VDR, may play a role. As this was not the case, genotype was disregarded in further analysis. Another interesting approach to this topic could be further investigation into the interaction between genetics and CKD progression. CKD is ultimately associated and characterized by the development of fibrosis, this also being a prognostic indicator regardless of underlying primary disease. The underlying molecular pathways that lead to renal interstitial fibrosis in progressing CKD have been thoroughly researched in recent years, however little is known about the greatly different course of progression in individual patients. A potential starting point for therapeutic approaches could be to examine how genetics or even epigenetics interacts with the development of fibrosis during the advancement of CKD (Tampe and Zeisberg 2014).

Noticeable was the seeming appearance of more fibrosis in --/-- NX_V mice. Upon closer evaluation of error bars, this increase is of no significance as the data of these mice is comparable to other NX_V genotypes as well. A possible explanation for a similar effect could be that this group of mice was more severely operated, meaning that more organ mass could have been unintentionally removed in comparison to other groups. This was not the case in this experiment, though, as remaining kidney mass was calculated for all animals and was comparable between groups. Another possibility could be that these mice had preexisting renal pathologies due to the open cage housing and therefore a potential contamination risk. However, this is rather unlikely as the --/-- SH data lies within the same range as the other SH groups. A potentially interesting development would have been if both --/-- NX_V and NX_AB groups had displayed an increase in fibrosis, as this could have indicated that genotype may indeed play a significant role. However, as this was not the case, the appearance of increased fibrosis for this particular group was disregarded.

The evaluation of the PSR results also showed no significant effect of FGF23 antibody treatment or surgery on the amount of renal fibrosis. Based on current literature as mentioned above, these results were unexpected and could have several possible explanations. Regarding the factor surgery, it is possible that the mice were not operated extremely enough during the 5/6 NX, meaning that not enough functional kidney mass was removed. As mentioned above already, this is unlikely as remaining kidney mass was calculated for all animals. When considering the effect of FGF23 antibody application, a possible explanation could be that this time period was not sufficiently long enough for collagen to begin to degrade to some extent, as the overall time between antibody application and euthanization was only four hours. An interesting approach would be to allow for a longer amount of time following antibody application, in order to assess if the results are time related as well as analyze any potential morphological changes in kidney parenchyma that could indicate a reduced amount of fibrosis. As the questions in this experiment were very diverse and the tissue samples were later also used for molecular biology purposes, one could also look at collagen markers at the mRNA level, as these may have already reacted in comparison to PSR staining. In general, also worth mentioning is the small group size, with n = 5. Larger groups would have been desirable for this study to have more statistical power, however the practicality of this

considering the number of different groups would have been difficult. As I also had no prior experience with the evaluation of PSR staining, it was challenging to set accurate threshold values when working with the Image J software – this is essential to correctly analyze PSR staining and gather accurate data. Another factor could have been that the PSR slides lost signal intensity in the period of time between staining and photographing. To minimize loss of signal, slides were therefore always stored in the dark.

To reiterate once again the function of the FGF23/klotho pathway: FGF23 plays an important role in regulating mineral homeostasis, especially vitamin D and phosphate metabolism. FGF23 transcription is influenced by vitamin D hormone and secretion can also be stimulated directly or indirectly by parathyroid hormone (PTH), phosphate, iron deficiency, proinflammatory cytokines, angiotensin II and aldosterone (Erben 2019). Klotho, a transmembrane protein, functions together with FGF receptor 1 as a receptor complex for FGF23 (Chen et al. 2018). As mentioned previously, klotho is mainly expressed in the kidney, as well as in the parathyroid and the choroid plexus of the cerebral ventricle. FGF23 and klotho are part of the same signaling pathway, which essentially functions as a safety net against hyperphosphatemia by increasing phosphate excretion, in addition to indirectly inhibiting intestinal phosphate absorption, as well as calcium absorption, by suppressing vitamin D hormone synthesis (Erben 2019). Recently, it has been increasingly observed that "progressive hyperphosphatemia, rising FGF23 levels and low Klotho expression are all observed in patients with progressive CKD and are associated with age-associated CVD [cardiovascular disease]" (Buchanan et al. 2020) (Hu et al. 2011).

To further investigate the behavior of klotho production in wt/wt, wt/-- and --/-- mice, as well as the effects of FGF23 inhibition in these respective groups, we also examined klotho protein expression via western blot analysis. It is well established that following a 5/6NX, there should be a decrease in klotho production (Aizawa et al. 1998). The typical decrease in klotho production could be primarily due to the surgical removal of functional kidney tissue, as the kidneys are the primary source of transmembrane and soluble klotho expression (Kuro-o 2009, Erben 2019). Recent studies with animal models have also shown that a decline in klotho can be correlated to CKD progression (Buchanan et al. 2020, Lindberg et al. 2014).

The decrease in klotho expression could therefore also be alternatively attributed to a CKD associated dysfunctional FGF23/klotho signaling pathway.

Preliminarily, we can see that the results confirm that our VDR/klotho knockouts were successful, as klotho intensity is very minimal in the --/-- SH group and even less in the NX group. We then analyzed the effect of surgical procedure alone. Evaluation revealed that 5/6NX did not significantly lower the expression of klotho, regardless of genotype. However, when looking at the graphs, we can see a noticeable difference. Based on previous studies as mentioned above, we therefore assume that our results are most likely a result of too few animals per group, as statistical testing does not reach significance ($p < 0,01$). Our results also indicate that following a 5/6 nephrectomy, the mechanisms underlying klotho expression could possibly be independent of vitamin D metabolism and receptors, since the wt/wt and wt/-- groups show very minimal differences in klotho intensity.

To further explore the pathophysiological underpinnings of CKD associated upregulated FGF23, we examined our murine CKD model in combination with an anti-FGF23 antibody treatment in order to pharmacologically induce acute loss FGF23 signaling. As can be seen in our results, the anti-FGF23 antibody had no significant effect on the wt/wt group. Though the difference in klotho intensity in the --/-- group is statistically significant, we have considered it as biologically irrelevant as the actual amount of klotho is minimal. Interestingly, the wt/-- group showed a significant increase in klotho production after FGF23 antibody application. This implies that there is an FGF23 driven and VDR dependent regulation of klotho in NX animals. High levels of FGF23 could therefore be responsible for a decline in klotho in wt/-- mice, however this seems unlikely as the wt/wt also display a similar klotho decrease. Further research would be necessary to determine if there are other potential factors that influence the decrease of klotho expression in wt/wt mice. In general, it must also be mentioned that increasing group size would provide more powerful data und insight. It might also be of significance to allow for a longer amount of time following antibody application, in order to assess if the results are time related as well.

5. Summary

Currently, chronic kidney disease poses an increasingly relevant health risk as the disease affects 10 % of adults worldwide. Chronic kidney disease leads to irrevocable damage to kidney tissue that can ultimately result in kidney failure and numerous other systemic complications. In recent years it has become clear that changes in fibroblast growth factor-23 secretion, as well as renal klotho expression, are central elements in the pathophysiology of chronic kidney disease. An increase of intact fibroblast growth factor-23 in blood concentrations is one of the earliest changes associated with the progression and development of chronic kidney disease. It has also been shown that elevated circulating fibroblast growth factor-23 in chronic kidney disease patients is not only associated with disease progression, but also with left ventricular hypertrophy and mortality. The fibroblast growth factor-23/klotho axis is not only a significant pathogenic contributor to the progression of chronic kidney disease; it is also a crucial tool for diagnostic and prognostic purposes. This makes it an extremely interesting target for therapeutic approaches; however, the exact pathophysiological mechanisms behind this signaling pathway must be further investigated. This work aims to explore the underlying molecular mechanisms of the fibroblast growth factor-23/klotho axis and its role in the pathophysiology of chronic kidney disease. Utilizing molecular biological methods, specifically western blotting, it was investigated how chronic kidney disease affects different genotypes. We also examined the effects of pharmacologically induced fibroblast growth factor-23 inhibition by way of an anti-fibroblast growth factor-23 antibody. Additionally, the role of fibroblast growth factor-23 in related renal fibrosis using histological methods including picrosirius red staining of kidney sections was studied. Murine C57BL/6 models with varying genotypes (wild type, vitamin-D-receptor knockout and vitamin-D-receptor/klotho knockout) were used and divided into groups based on type of surgery and treatment. Chronic kidney disease in the models was induced by way of a 5/6 nephrectomy. The results of this study indicate that fibroblast growth factor-23 plays a crucial role in the pathology of chronic kidney disease and subsequent mineral homeostasis abnormalities. Interestingly, there may also be a fibroblast growth factor-23 driven and vitamin-D-receptor dependent regulation of klotho, however, further research is necessary.

6. Zusammenfassung

Die chronische Nierenerkrankung ist eine fortschreitende und meist irreversible Beeinträchtigung der Nierenfunktion, die letztendlich zu Nierenversagen und einer Reihe weiterer systemischer Komplikationen führt. Derzeit stellt die chronische Nierenerkrankung ein zunehmend relevantes Gesundheitsrisiko dar, da die Krankheit weltweit 10 % der Erwachsenen betrifft. Diese Arbeit beschäftigt sich mit den zugrunde liegenden molekularen Mechanismen der Fibroblasten-Wachstumsfaktor 23/Klotho-Achse und ihrer Rolle in der Pathophysiologie chronischer Nierenerkrankungen. Mit molekularbiologischen Methoden, insbesondere Western Blotting, habe ich die Auswirkung der chronischen Niereninsuffizienz auf verschiedene Genotypen untersucht und analysierte auch die Auswirkungen einer pharmakologisch induzierten Hemmung des Fibroblasten-Wachstumsfaktors 23. Darüber hinaus untersuchte ich die Rolle vom Fibroblasten-Wachstumsfaktor 23 bei verwandter Nierenfibrose mit histologischen Methoden, einschließlich der „Picrosirius Red“ Färbung von Nierenschnitten. Dafür wurden murine C57BL/6-Modelle mit unterschiedlichen Genotypen (Wild type, Vitamin-D-Rezeptor-Knockout und Vitamin-D-Rezeptor/Klotho-Knockout) verwendet und, basierend auf der Art der Operation und Behandlung, in Gruppen eingeteilt. In den Modellen wurde eine chronische Niereninsuffizienz durch eine 5/6-Nephrektomie induziert. Die Ergebnisse der Studie weisen darauf hin, dass der Fibroblasten-Wachstumsfaktor 23 eine entscheidende Rolle bei der Pathologie chronischer Nierenerkrankungen und nachfolgender Anomalien der Mineralhomöostase spielt. Es gibt auch Hinweise auf eine Fibroblasten-Wachstumsfaktor 23-gesteuerte und Vitamin-D-Rezeptor-abhängige Regulation von Klotho, für eine Verifikation sind jedoch weitere Untersuchungen erforderlich.

7. List of Abbreviations

ANOVA	analysis of variance
BCA	bicinchoninic acid
BSA	bovine serum albumin
CKD	chronic kidney disease
FGF23	fibroblast growth factor 23
FGF23AB	fibroblast growth factor 23 antibody
GFR	glomerular filtration rate
Klotho	α-klotho
NX	5/6 nephrectomized
PSR	picrosirius red staining
PTH	parathyroid hormone
RD	rescue diet
RIPA	radioimmunoprecipitation assay buffer
SDS-PAGE	sodium dodecyl sulfate – polyacrylamid gel electrophoresis
SEM	standard error of mean
SH	sham operated
SNK	student-newman-keuls
TRPV5	transient receptor potential channel subfamily vanilloid 5
VDR	vitamin D receptor
WNK	with–no-lysine kinases

8. List of References

Aizawa H., Saito Y., Nakamura T., et al. 1998. Downregulation of the Klotho gene in the kidney under sustained circulatory stress in rats. *Biochemical and Biophysical Research Communications.* 28;249(3):865-71. DOI 10.1006/bbrc.1998.9246 (Accessed on 13.10.2022).

Andrukhova O., Zeitz U., Goetz R., et al. 2012. FGF23 acts directly on renal proximal tubules to induce phosphaturia through activation of the ERK1/2-SGK1 signaling pathway. *Bone*. 51(3):621-628. DOI 10.1016/j.bone.2012.05.015 (Accessed on 12.09.2020).

Andrukhova O., Slavic S., Smorodchenko A., et al. 2014. FGF23 regulates renal sodium handling and blood pressure. *EMBO Molecular Medicine*. 6(6):744-759. DOI 10.1002/emmm.201303716 (Accessed on 12.09.2020).

Andrukhova O., Schüler C., Bergow C., et al. 2018. Augmented Fibroblast Growth Factor-23 Secretion in Bone Locally Contributes to Impaired Bone Mineralization in Chronic Kidney Disease in Mice. *Frontiers in Endocrinology (Lausanne).* 9:311. DOI 10.3389/fendo.2018.00311 (Accessed on 15.09.2020).

Bao Y.W., Yuan Y., Chen J.H., et al. 2018. Kidney disease models: tools to identify mechanisms and potential therapeutic targets. *Zoological Research.* 18;39(2):72-86. DOI 10.24272/j.issn.2095-8137.2017.055 (Accessed on 06.10.2020).

Bartges J. W., 2012. Chronic kidney disease in dogs and cats. *The Veterinary Clinics of North America Small Animal Practice.* 42(4):669-vi. DOI 10.1016/j.cvsm.2012.04.008 (Accessed on 08.09.2020).

Buchanan S., Combet E., Steinvinkel P., et al. 2020. Klotho, Aging, and the Failing Kidney. *Frontiers in Endocrinology*. 11:560. DOI 10.3389/fendo.2020.00560 (Accessed 01.06.2022).

Chakrabarti S., Syme H.M., Elliott J. 2012. Clinicopathological variables predicting progression of azotemia in cats with chronic kidney disease. Journal of Veterinary Internal Medicine. 26(2):275–281. DOI 10.1111/j.1939-1676.2011.00874.x (Accessed 23.11.2021).

Chen G., Liu Y., Goetz R., et al. 2018. α-Klotho is a non-enzymatic molecular scaffold for FGF23 hormone signaling. *Nature.* 553(7689):461-466. DOI 10.1038/nature25451 (Accessed on 10.09.2020).

Cho M. H. 2010. Renal fibrosis. *Korean Journal of Pediatrics*. 53(7):735-40. DOI 10.3345/kjp.2010.53.7.735 (Accessed on 05.10.2020).

Eckardt K.U., Coresh J., Devuyst O., et al. 2013. Evolving importance of kidney disease: from subspecialty to global health burden. *Lancet*. 382(9887):158-169. DOI 10.1016/S0140-6736(13)60439-0 (Accessed on 15.09.2020).

Erben, R.G. 2019. Physiologie und Pathophysiologie von FGF23 und Klotho. *Nephrologe*. 14, 302–304. DOI 10.1007/s11560-019-0344-9 (Accessed on 10.09.2020).

Erben R.G., Soegiarto D.W., Weber K., et al. 2002. Deletion of deoxyribonucleic acid binding domain of the vitamin D receptor abrogates genomic and nongenomic functions of vitamin D. *Molecular Endocrinology*. 16(7):1524-1537. DOI 10.1210/mend.16.7.0866 (Accessed on 07.09.2020).

Gäbel G., Fromm M. 2015. Niere, In: Engelhardt et al. Hrsg. Physiologie der Haustiere. 5. Auflage, Stuttgart: Enke, 299 – 324.

GBD 2015 Disease and Injury Incidence and Prevalence Collaborators. 2016. Global, regional, and national incidence, prevalence, and years lived with disability for 310 diseases and injuries, 1990-2015: a systematic analysis for the Global Burden of Disease Study. *Lancet*. 388(10053):1545-1602. DOI 10.1016/S0140-6736(16)31678-6 (Accessed on 08.09.2020).

Gille U. 2008. Harn- und Geschlechtsapparat, *Apparatus urogenitalis*. In: Salomon F, Geyer H, Gille U. Hrsg. Anatomie für die Tiermedizin. 2. Auflage. Stuttgart: Enke, 370 – 378.

Hnasko T.S., Hnasko R.M. 2015. The Western Blot. *Methods in Molecular Biology*. 1318:87-96. DOI 10.1007/978-1-4939-2742-5_9 (Accessed 01.09.2020).

Hoorn E.J., Nelson J.H., McCormick J.A., et al. 2011. The WNK kinase network regulating sodium, potassium, and blood pressure. *Journal of the American Society of Nephrology*. 22(4):605-614. DOI 10.1681/ASN.2010080827 (Accessed on 12.09.2020).

Hu M.C., Shiizaki K., Kuro-o M., et al. 2013. Fibroblast growth factor 23 and Klotho: physiology and pathophysiology of an endocrine network of mineral metabolism. *The Annual Review of Physiology*. 75:503-533. DOI 10.1146/annurev-physiol-030212-183727 (Accessed on 09.09.2020).

Hu M.C., Shi M., Zhang J., et al. 2011. Klotho deficiency causes vascular calcification in chronic kidney disease. *Journal of the American Society of Nephrology.* 22(1):124-36. DOI 10.1681/ASN.2009121311 (Accessed on 21.12.2022).

Isakova T., Xie H., Yang W., et al. 2011. Fibroblast growth factor 23 and risks of mortality and end-stage renal disease in patients with chronic kidney disease. *Journal of the American Medical Association*. 305(23):2432-2439. DOI 10.1001/jama.2011.826 (Accessed on 12.09.2020).

Isakova T., Wahl P., Vargas G.S., et al. 2012. Fibroblast growth factor 23 is elevated before parathyroid hormone and phosphate in chronic kidney disease. *Kidney International*. 79(12):1370-1378. DOI 10.1038/ki.2011.47 (Accessed on 12.09.2020).

Kuro-o M., Matsumura Y., Aizawa H., et al. 1997. Mutation of the mouse klotho gene leads to a syndrome resembling ageing. *Nature*. 390(6655): 45-51. DOI 10.1038/36285 (Accessed on 11.10.2020).

Kuro-o M. 2019. Klotho and aging. *Biochimica et Biophysica Acta*. 1790(10): 1049-1058. DOI 10.1016/j.bbagen.2009.02.005 (Accessed on 18.05.2022).

Kurosu H., Ogawa Y., Miyoshi M., et al. 2006. Regulation of fibroblast growth factor-23 signaling by klotho. *Journal of Biological Chemistry*. 281(10):6120-6123. DOI 10.1074/jbc.C500457200 (Accessed on 10.09.2020).

Laemmli U.K. 1970. Cleavage of structural proteins during the assembly of the head of bacteriophage T4. *Nature*. 227(5259):680-685. DOI 10.1038/227680a0 (Accessed on 31.08.2020).

Lattouf R., Younes R., Lutomski D., et al. 2014. Picrosirius red staining: a useful tool to appraise collagen networks in normal and pathological tissues. *Journal of Histochemistry and Cytochemistry*. 62(10):751-758. DOI 10.1369/0022155414545787 (Accessed 22.08.2020).

Lau W. L., Linnes M., Chu E. Y., et al. 2013. High phosphate feeding promotes mineral and bone abnormalities in mice with chronic kidney disease. *Nephrology Dialysis Transplantation*. 28(1):62-9. DOI 10.1093/ndt/gfs333 (Accessed on 23.09.2022).

Lim B., Yang H., Fogo A. 2014. Animal models of regression/progression of kidney disease. *Drug discovery today. Disease models*, 11, 45–51. DOI 10.1016/j.ddmod.2014.06.003 (Accessed 01.08.2020).

Lindberg K., Amin R., Moe O.W., et al. 2014. The kidney is the principal organ mediating Klotho effects. *Journal of the American Society of Nephrology.* 25:2169–75. DOI 10.1681/ASN.2013111209 (Accessed on 01.06.2022).

Maique J., Flores B., Shi M., et al. 2020. High Phosphate Induces and Klotho Attenuates Kidney Epithelial Senescence and Fibrosis. *Frontiers in Pharmacology.* 11:1273. DOI 10.3389/fphar.2020.01273 (Accessed 21.12.2022).

Marino C.L., Lascelles B.D., Vaden S.L., et al. 2014. Prevalence and classification of chronic kidney disease in cats randomly selected from four age groups and in cats recruited for degenerative joint disease studies. *Journal of Feline Medicine and Surgery.* 16(6):465–472. DOI 10.1177/1098612X13511446 (Accessed 23.11.2021).

Martin A., David V., Quarles L.D., 2012. Regulation and function of the FGF23/klotho endocrine pathways. *Physiological Reviews.* 92(1):131-155. DOI 10.1152/physrev.00002.2011 (Accessed on 10.09.2020).

Miao J., Huang J., Luo C., Ye H., et al. 2021. Klotho retards renal fibrosis through targeting mitochondrial dysfunction and cellular senescence in renal tubular cells. *Physiological Reports*. 9(2):e14696. DOI 10.14814/phy2.14696 (Accessed 21.12.2022).

Montes G.S., Junqueira L.C., 1991. The use of the Picrosirius-polarization method for the study of the biopathology of collagen. *Memórias do Instituto Oswaldo Cruz*. 86 Suppl 3:1-11. DOI 10.1590/s0074-02761991000700002 (Accessed 22.08.2020).

O'Neill D.G., Elliott J., Church D.B., et al. 2013. Chronic kidney disease in dogs in UK veterinary practices: prevalence, risk factors, and survival. *Journal of Veterinary Internal Medicine*. 27(4):814-821. DOI 10.1111/jvim.12090 (Accessed 10.09.2020).

Radloff J., Latic N., Pfeiffenberger U., et al. 2021. A phosphate and calcium-enriched diet promotes progression of 5/6-nephrectomy-induced chronic kidney disease in C57BL/6 mice. *Scientific Reports*. 11(1):14868. DOI 10.1038/s41598-021-94264-8 (Accessed on 23.09.2022).

Rodelo-Haad C., Santamaria R., Muñoz-Castañeda J.R., et al. 2019. FGF23, Biomarker or Target? *Toxins (Basel).* 11(3):175. DOI 10.3390/toxins11030175 (Accessed on 09.09.2020).

Shimada T., Hasegawa H., Yamazaki Y., et al. 2004. FGF-23 is a potent regulator of vitamin D metabolism and phosphate homeostasis. *Journal of Bone and Mineral Research.* 19(3):429-435. DOI 10.1359/JBMR.0301264 (Accessed on 10.09.2020).

Smith P.K., Krohn R.I., Hermanson G.T., et al. 1985. Measurement of protein using bicinchoninic acid. *Analytical biochemistry*. 150(1):76-85. DOI 10.1016/0003-2697(85)90442-7 (Accessed on 31.08.2020).

Tampe B., Zeisberg M. 2014. Contribution of genetics and epigenetics to progression of kidney fibrosis. *Nephrology Dialysis Transplantation.* 29 Suppl 4:iv72-9. DOI 10.1093/ndt/gft025 (Accessed on 15.10.2020).

Wang Y., Borchert M.L., DeLuca H.F. 2012. Identification of the vitamin D receptor in various cells of the mouse kidney. *Kidney International*. 81(10):993-1001. DOI 10.1038/ki.2011.463 (Accessed on 13.10.2020).

Webster A.C., Nagler E.V., Morton R.L., et al. 2017. Chronic Kidney Disease. *Lancet*. 389(10075):1238-1252. DOI 10.1016/S0140-6736(16)32064-5 (Accessed on 08.09.2020).

Wu Y.L., Xie J., An S.W., et al. 2017. Inhibition of TRPC6 channels ameliorates renal fibrosis and contributes to renal protection by soluble klotho. *Kidney International*. 91(4):830-841. DOI 10.1016/j.kint.2016.09.039 (Accessed on 21.12.2022).

Zhang Q.L., Rothenbacher D. 2008. Prevalence of chronic kidney disease in population-based studies: systematic review. *BMC Public Health*. 8:117. DOI 10.1186/1471-2458-8-117 (Accessed 08.09.2020).

Zehnder D., Hewison M. 1999. The renal function of 25-hydroxyvitamin D3-1alpha-hydroxylase. *Molecular and Cellular Endocrinology*. 151(1-2):213-220. DOI 10.1016/s0303-7207(99)00039-8 (Accessed on 12.09.2020).

9. List of Figures and Tables

Fig. 7: Graphical bar chart comparison of klotho antibody protein expression in intensity (%) after western blot quantification of target protein according to genotype **A)** wt/wt, **B)** wt/-- or **C)** --/-- in 5/6 nephrectomized (NX) mice. Vehicles were compared to mice treated with anti-FGF23 antibody (NX AB). Statistical analysis was performed via an unpaired T-Test. Presented data is shown as mean ± SEM with 4-6 animals in each group. ** $P < 0,01$.

Fig. 8: Sample excerpt of relative klotho protein expression in western blot analysis. Bands are labeled according to genotype (wt/wt, wt/--, --/--), surgery type (SH or NX) and treatment (FGF23AB). **A)** Comparison of klotho expression in SH or NX animals of all genotypes. **B)** Comparison of NX animals treated with FGF23AB of all genotypes to SH or NX vehicle animals of genotypes wt/wt and wt/--. **C)** Comparison of vehicles and FGF23AB treated animals that were NX operated of all genotypes. **D)** Comparison of NX FGF23 animals of all genotypes.

Tab. 1: Overview of experimental setup

Tab. 2: Dyes, solvents and powders used for histological processing and staining

Tab. 3: Overview of dewaxing protocol

Tab. 4: Overview of PSR staining protocol

Tab. 5: Equipment for SDS-PAGE

Tab. 6: Materials for SDS-PAGE

Tab. 7: Equipment and material for western blotting

Tab. 8: Overview of antibodies for immunodetection